Actomyosin Regulatory Properties of Yeast Tropomyosin Are Dependent upon N-Terminal Modification†

R. Maytum,*,‡ M. A. Geeves,‡ and M. Konrad§

Department of Biosciences, University of Kent at Canterbury, Canterbury, U.K., and Max-Planck-Institut fur Biophysikalische Chemie, Am Fassberg 11, D-37070 Göttingen, Germany

Received April 27, 2000; Revised Manuscript Received July 3, 2000

ABSTRACT: The yeast tropomyosin 1 gene (*TPM1*) encodes the major isoform of the two tropomyosins (Tm) found in yeast. The gene has been expressed in *E. coli* and the protein purified. The gene product (yTm1) is a 199-amino acid protein that has a low affinity for actin compared to the native yTm1 purified from yeast. Mass spectrometry shows that the native protein is acetylated while the recombinant protein is not. A series of yTm1 N-terminal constructs were made with either an Ala-Ser dipeptide extension previously shown to restore actin binding to skeletal muscle Tm or the natural extension found in fibroblast Tm 5a/b. All constructs bound actin tightly and showed similar CD spectra and thermal stability. All constructs induced cooperativity in the equilibrium binding of myosin subfragment 1, to actin but the binding curves differed significantly between the constructs. The apparent cooperative unit size (*n*) and closed/open equilibrium (K_T) were determined using a fluorescence titration technique [Maytum et al. (1998) *Biophys. J. 74*, A347]. The data could be accounted for by changes in K_T (0.1−1) with no change in *n*. Values of *n* were approximately twice the structural unit size (5 actin sites). The presence of yTm on actin had little effect upon the overall affinity of S1 for actin despite showing an ability to regulate the acto−myosin interaction. These results show that the short yTm can aid our understanding of actomyosin regulation and that the N-terminus of Tm has a major influence upon its regulatory properties.

Tropomyosin (Tm)[1] has been identified in eukaryotic cells ranging from yeast to man and appears to be as ubiquitous as the presence of actin and myosin. In yeast (*Saccharomyces cerevisiae*), the simplest system in which it has been identified, there are two Tms produced by two separate genes, *TPM1* and *TPM2*, present as single exons (*1*, *2*). The yeast tropomyosins, yTm1 and yTm2, are the shortest so far identified, comprising 199 or 161 amino acids, respectively, which is equivalent to 5 or 4 actin-binding sites (*1*). All other isoforms currently identified in the database (SwissProt − total 60 entries) have either approximately 248 or 284 amino acids, spanning 6 or 7 actins, respectively. The cellular roles of the two tropomyosins in yeast remain unclear. Gene knockouts have shown that double knockouts are lethal, lack of *TPM2* causes little phenotypic effect (probably due to complementation by *TPM1*), and cells lacking *TPM1* show poor growth and morphogenic problems (*2*). *TPM1* is involved with the structural regulation of actin filaments used in the Myo2p (a type V myosin) mediated trafficking of secretory vesicles and polarization of growth (*3*). It is not clear whether the physiological roles of these tropomyosins are purely structural or if they also have direct actin regulatory functions. The physiological role of nonmuscle Tms in higher organisms remains similarly undefined.

In muscle cells Tm has a well-defined regulatory function. The binding of Tm to the actin filament confers cooperativity upon the interaction with myosin heads and in combination with troponin (Tn) regulates striated muscle contraction (*4*). The $Actin_7Tm$ (A_7Tm) structural repeat unit of skeletal muscle thin filament has been used as the underlying cooperative unit in most models of thin filament regulation (e.g. refs *5*, *6*). However, recent evidence suggests that the apparent cooperative unit size for some forms of Tm (fibroblast 5a and smooth muscle Tm) is considerably greater than the structural repeat unit (*7*). This work suggested that this is due to strengthened end-to-end interactions between tropomyosins in the A_6Tm (fibroblast) or A_7Tm (smooth muscle) structural repeat. Evidence of enhanced Tm−Tm contacts producing longer range cooperativity has been well-established for skTm but only in the presence of Tn or more specifically the TnT_1 fragment of TnT which is thought to bind to the Tm−Tm overlap region (*7*−*9*). Current views of the thin filament regulation in striated muscle, based on both biochemical and structural data, suggest that Tm can occupy three different positions or states on actin (*6*, *10*). These have been termed the blocked, closed, and open states of the actin.Tm filament. To date the blocked state has only been observed for skeletal muscle A_7TmTn filaments in the absence of calcium.

We have recently developed a sensitive fluorescence titration method that uses nanomolar concentrations of pyrene-labeled actin stabilized by phalloidin. Titrating the

† R.M. and M.A.G. were supported by Welcome Trust Grant 055841, and M.K. was supported by the Max Planck Institute.

* To whom correspondence should be addressed. Tel: +44 1227 823950. Fax: +44 1227 763912. E-mail: rmm@ukc.ac.uk.

‡ University of Kent at Canterbury.

§ Max-Planck-Institut fur Biophysikalische Chemie.

[1] Abbreviations: Tm, tropomyosin; S1, myosin subfragment 1; yTm1, yeast tropomyosin 1; skTm, skeletal tropomyosin; smTm, smooth muscle tropomyosin; PCR, polymerase chain reaction; ATP adenosine triphosphate; Tn, troponin; TnT, troponin subfragment T; MOPS, 4-morpholinepropanesulfonic acid.

10.1021/bi000977g CCC: $19.00
Published on Web 09/07/2000

actin with myosin S1 allowed the determination of the cooperative, sigmoidal binding curves of S1 to actin with sufficient accuracy to fit to a model which incorporates cooperativity beyond the A_7Tm structural unit of the skTm used (*11*). These data confirmed that although the apparent cooperative unit size for skTm alone ($n = 7-8$) was close to that of its structural unit size, the addition of Tn in the presence of calcium caused an increase to significantly larger ($n = 11-12$) than the structural unit. The data also established that it was possible to determine the equilibrium constant, K_T, between the closed and open states of the thin filament.

We set out to use the above method to study the influence of yTm on the interaction between actin and myosin. Yeast tropomyosin 1 (*TPM1*) was expressed in *E. coli*. The purified recombinant protein (yTm1) shows similar properties to that of skTm expressed in bacteria in that it has an extremely low affinity for actin (*12*). For skTm this low affinity is known to be due to the absence of N-terminal acetylation of the protein in the bacterial expression system (*13*). We show that in contrast to the recombinant protein, yTm1 purified from yeast is natively acetylated.

It has been shown that short N-terminal extensions of the Tm can restore normal actin binding. We have therefore made N-terminal constructs of yTm and measured their actin affinity and conformational stability which showed all to be nativelike. We report here a detailed characterization of S1 binding to actin filaments containing the expressed yTm constructs which allowed determination of the apparent cooperative unit size (n) and equilibrium constant (K_T) for the closed to open transition. These measurements show both that yTm is capable of regulating the acto−myosin interaction and that small variations in the N-terminal sequences can have a dramatic effect upon the regulatory properties of the yTm.

Some of this work has been reported in a preliminary form (*14*).

MATERIALS AND METHODS

DNA Constructs. General recombinant DNA techniques were performed as described in Sambrook et al. (*15*) or as recommended by the supplier.

Yeast *TPM1* was cloned from total yeast genomic DNA by standard PCR using Taq polymerase (Roche Molecular Biochemicals) with primers designed to match the N- and C-terminal coding regions and including *Nde*I and *Bam*HI (*italic*) subcloning sites, respectively, for insertion into the pJC20 expression vector (*16*). The sequences used for the primers were as follows: 5′-GGGCC*CAT ATG* GAC AAA ATC AGA GAA AAG CTA-3′ (5′-forward primer) and 5′-CCCTT*GGA TCC* TCA CAA GTT TTC CAG AGA TGC AGC-3′ (3′-reverse primer). The 0.6-kb PCR product was cut with *Nde*I and *Bam*HI, ligated into pJC20, and transformed into the *E. coli* strain XL1-Blue. *TPM1* mutants were produced by PCR using combinations of the 3′ reverse *TPM* primer along with 5′ primers including the modified sequences (underlined) for the 5′ terminus (see Figure 1). The 5′ primers were designed as for the original primer to include the *Nde*I site for cloning into the expression vector. The sequences for the primers used were as follows: *TPM1(n2)* 5′-GGAATTC*CAT ATG* GCG AGC ATG GAC AAA ATC AGA GAA AAG C-3′, *TPM1(n5)* 5′-GGAATTC*CAT ATG* GCG GGT AGC AGC TCT ATG GAC AAA ATC AGA GAA AAG C-3′, *TPM1(n9)* 5′-GGAATTC*CAT ATG* GCG GGT AGC AGC TCG CTG GAG GCG GTG AGA GAA AAG CTA AGC AAC TTG AAG-3′.

Tm 5a/b	**(M)** AGSSSLEAV**R**R**K**IR**S**
yTm1	**MDKIREKLSN**
yTm1(n2)	**(M)** AS**MDKIREKLSN**
yTm1(n5)	**(M)** AGSSS**MDKIREKLSN**
yTm1(n9)	**(M)** AGSSSLEAV**REKLSN**

FIGURE 1: (Top) N-Termini of a sequence alignment of fibroblast Tm 5a/b and yTm1. (Bottom) Three N-terminal mutants of yTm1 produced, with the alterations being shown in normal typeface. The n2 mutant is based on the previously published dipeptide used for skTm, while the n5 and n9 mutants are based upon the first 6 or 10 residues of the fibroblast Tm 5a/b sequence. The N-terminal methionines (in brackets) are removed by posttranscriptional processing.

The entire coding regions of the mutants were verified by automatic DNA sequencing (Applied Biosystems 373 sequencer) using a dye-based PCR sequencing reaction.

Protein Expression and Purification. For protein expression the purified plasmid was transformed into competent BL21(DE3) pLys cells and plated for colony isolation. Several single colonies were picked from each and inoculated into 5 mL of LB medium containing 100 mg/L ampicillin for trial expression. When $OD_{600\ nm}$ of about 0.6 was reached, new cultures were started from each and the remainder induced with 0.4 mM IPTG. Cells were then grown for 3 h at 37 °C and 0.5-mL samples harvested and run on SDS gels to check expression levels. Cultures showing good levels of expression were then used to seed 1-L cultures for protein production.

Cultures were grown to late exponential phase and induced for 3 h with 0.4 mM IPTG. Cells were harvested by centrifugation at 6000 rpm Sorvall GS-3 rotor, resuspended in 60 mL of lysis buffer (20 mM Tris pH 7.5, 100 mM NaCl, 2 mM EDTA, 1 mg/L DNAse, 1 mg/L RNAse) and lysed by passage through a cell disrupter 5−6 times. The samples were then heated to 80 °C for 10 min and spun at 10k rpm, Sorvall GSA to pellet precipitated protein and cell debris. The soluble Tm was then isoelectrically precipitated from the supernatant by careful adjustment of the pH to 4.5 using 0.3 M HCl. After 15 min the precipitate was pelleted (10k, Sorvall SS-34) and resuspended in 10−20 mL (dependent upon yield) of running buffer (10 mM phosphate pH 7.0, 100 mM NaCl, the pH readjusted after the pellet was dissolved). This was then further purified using a 6-mL Pharmacia Resource-Q column, eluted with a 150−400 mM NaCl gradient, the Tm eluting at around 200−250 mM salt. Fractions were analyzed by SDS−PAGE, pooled and concentrated by isoelectric precipitation. Purity was checked by SDS−PAGE and comparison of 280/260 nm absorbance ratio. If the sample was insufficiently pure (normally nucleotide contamination) it was subjected to a second column purification step identical to the first. Yeast Tm protein concentrations were estimated using an extinction coefficient $E^{1\%}$ of 6.0 cm^{-1} calculated from the sequences using AnTheProt (Gilbert Deleage, IBCP−CNRS).

Purification of Native Yeast Tropomyosin. Native yeast tropomyosin was prepared directly from yeast cake (gift from Asda Group plc). 50 g wet weight yeast cake was resus-

pended in 75 mL of cold lysis buffer (20 mM Tris pH 7.5, 300 mM KCl, 20 mM EDTA, 1 mM $MgCl_2$, 0.3 mM PMSF, 0.5 mM benzamidine, 1 mM DTT). The suspension was then lysed by passage through a French press and immediately heated to 90 °C for 15 min. All subsequent steps were identical to those detailed above for purification of the recombinant protein.

Electrospray Mass Spectrometry. Protein molecular weight was determined by electrospray mass spectrometry. For this, small (50-μL) stock samples were dialyzed overnight against 1 mM Tris pH 7.0, acidified with formic acid and applied to a Finnegan Mat LCQ ion-trap MS fitted with a nanospray device. Mass accuracy for yTm samples is expected to be 2−3 Da (1/10 000). Predicted molecular weights for proteins were calculated using AnTheProt (Gilbert Deleage, IBCP-CNRS) with Delta Mass (ABRF) used to determine mass differences due to modifications.

Other Proteins and Reagents. Myosin subfragment 1 (S1) was prepared by chymotryptic digestion of rabbit myosin, as described by Weeds and Taylor (*17*). Its molar concentration was calculated from absorbance measurement at 280 nm using an $E^{1\%}$ of 7.9 cm^{-1} and a molecular weight of 115 000 Da. Rabbit actin was purified by the method of Spudich and Watt (*18*). Its molar concentration was determined by its absorbance at 280 nm using an $E^{1\%}$ of 11.08 cm^{-1} and a molecular weight of 40 000 Da. The preparation of pyrene-labeled actin (pyr-actin) was as previously described (*19*). Phalloidin (Boehringer) stabilized F-actin was made by incubating a solution of 10 μM pyrene-actin with 10 μM phalloidin overnight in experimental buffer (20 mM MOPS pH 7.0, 200 mM KCl, 5 mM $MgCl_2$) at 4 C.

CD and Fluorescence Spectroscopy. CD spectra were measured using 0.5 mg/mL samples of protein in 10 mM sodium phosphate pH 7.0, 0.5 M NaCl, 5 mM $MgCl_2$, 1 mM DTT in a Jasco 600 CD spectrophotometer from 190 to 250 nm using a 0.5-mm cell at 20 °C. Samples were allowed to equilibrate for at least 5 min at each temperature. Folding/unfolding was fully reversible and repeat runs yielded identical results.

Fluorescence titrations were measured on an SLM 8100 spectrofluorimeter at 20 °C exciting at 365 nm with an 8-nm bandwidth and measuring emission at 405 nm with a 16-nm bandwidth. A total working volume of 2 mL was used in a 10- × 10-mm cell constantly stirred using a magnetic stirrer below the light path of the instrument. Autotitrations were made using a Harvard Apparatus syringe infusion pump 22 driving a 100-μL glass syringe (Hamilton) as described previously (*11*). Data were acquired over a period of 250 s, with data points being collected every 0.5 s, using an integration time of 0.45 s. Buffer solutions for the titrations were filtered using a 0.22-μm disposable syringe filter to remove dust particles which can produce significant noise in the stirred cell at the low levels of sample fluorescence used. Titrations are recorded with a continuous addition of a concentrated S1 stock solution into a continuously stirred cell using a syringe pump. The use of a 10- × 10-mm cell (2-mL volume) reduces the effects of dilution (only 50 μL in total is added during a titration) and fluorescence bleaching (only a small fraction of the continuously mixed solution is exposed to the light source at any time). Mixing and equilibration of the reaction in the cell were checked as detailed previously (*11*).

Quantitative Electrophoresis. SDS−Polyacrylamide gel electrophoresis (SDS−PAGE) was performed according to Laemmli (*20*) using 13.5% acrylamide gels and stained with Coomassie Blue G-250. Quantification of proteins was carried out by using a Mustek 1200-SP scanner with transparency adapter attached to a PC. The scanner was calibrated using a Kodak density step tablet, and scanned images were analyzed using the Image-PC program (Scion Corp. based upon NIH-Image).

Modeling. The equilibrium binding of S1 to unregulated actin conforms to a simple binding model with the dissociation constant K_d:

$$A + M \overset{K_d}{\longleftrightarrow} A{\cdot}M$$

It can therefore be shown that a titration of S1 against actin can be fitted to the physically significant root of the quadratic equation:

$$\alpha = \frac{([M] + K_d + [A]_0) - \sqrt{([M] + K_d + [A]_0)^2 - 4[M][A]_0}}{2[A]_0} \quad (1)$$

where α is the fraction of actin with S1 bound, [M] the total concentration of S1 added, and $[A]_0$ is the initial actin concentration.

Binding can be monitored by the quenching of a pyrene label attached to actin. The fraction of actin bound is then directly proportional to the change in fluorescence:

$$\alpha = \frac{F_0 - F}{F_0 - F_\infty} \quad (2)$$

In a system containing only tropomyosin, the blocked state of the three-state model (*6*) is assumed to be absent. A simpler two-state version (discarding the $1/K_B$ term) of the three-state equation from Maytum et al. (*11*) for a cooperative unit size n can therefore be used. K_1 (binding to the A state), K_2 (A to R isomerization), and K_T (the closed/open equilibrium) are as shown previously (*11*):

$$\alpha = \frac{K_1[M]P^{n-1}(K_T(1 + K_2)^n + 1)}{(K_T P^n + Q^n)(1 + K_2)^{n-1}} \quad (3)$$

where α is as defined in eq 2, [M] is in this case the concentration of free S1, $P = 1 + K_1[M](1 + K_2)$, and $Q = 1 + K_1[M]$.

RESULTS

Properties of Yeast TPM1. The *TPM1* gene from *S. cerevisiae* was successfully expressed in *E. coli.* The yield of purified protein was typically 20−30 mg from 1 L of cultured cells. The purified protein (yTm1) ran on SDS−PAGE at the anomalous molecular weight of 33 kDa as previously shown for the native protein (*21*). The CD spectrum of the purified protein shown in Figure 2A possessed the double minima at 208 and 222 nm characteristic of the correctly folded, fully α-helical structure of tropomyosins and was essentially identical to that of native rabbit muscle Tm. The binding of yTm1 to actin was

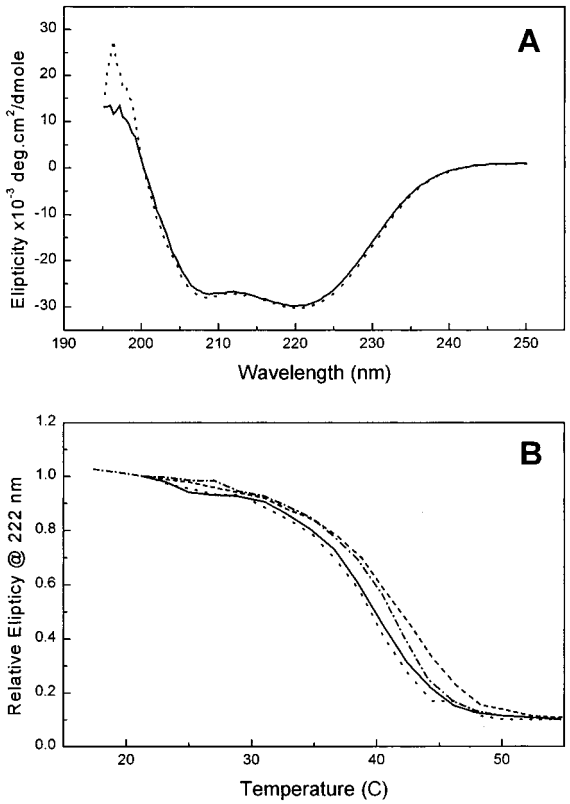

FIGURE 2: (A) Comparison of CD spectra of 0.5 mg/mL samples of native rabbit muscle tropomyosin and recombinant yTm1 measured from 190 to 250 nm in 10 mM phosphate pH 7.0, 500 mM KCl, 5 mM $MgCl_2$. (B) CD melting curves for yTm1 (solid), yTm1(n2) (dot), yTm1(n5) (dash), and yTm1(n9) (dot−dash). Melting spectra were measured in a 0.5-mm cell at 0.2 mg/mL in 10 mM $NaPO_4$ pH 7.0, 0.5 M NaCl, 1 mM EGTA, 1 mM DTT.

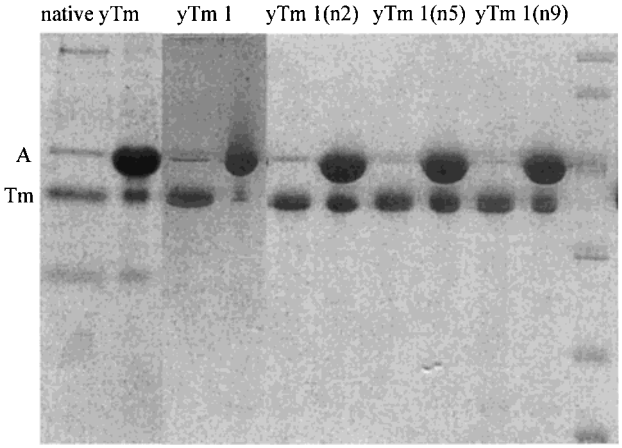

FIGURE 3: Cosedimentation of tropomyosins with actin. 20 μM actin was mixed with approximately 5 μM of each of the different yeast Tms in 20 mM MOPS pH 7.0, 5 mM $MgCl_2$, 200 mM KCl. The actin was then pelleted at 100000*g* for 20 min. Equivalent samples of the pellet and supernatant were run in parallel on SDS−PAGE (supernatant in left lane and pellet in right for each pair) and stained with Coomassie blue.

measured by cosedimentation studies (Figure 3) in which Tm was mixed with rabbit actin and the F-actin and any bound protein were pelleted by centrifugation. This showed little or no binding of yTm1 to the F-actin, with all of the Tm remaining unbound in the supernatant. Mass spectrometry of the purified recombinant protein (yTm1) gave a determined molecular weight of 23 544.5 Da, virtually identical to that calculated from the amino acid sequence for an unmodified protein of 23 541.8 Da; i.e. the N-terminal methionine is unmodified. By analogy to skTm this absence of acetylation may explain the low affinity of the expressed Tm for actin.

Native Yeast Characterization. Native yeast tropomyosin was isolated directly from wild-type cells. The yield of protein was similar to that previously reported (*21*) with 50 g (ww) of cells yielding around 1 mg of purified protein. The purified protein was assayed for actin binding as for the recombinant proteins and showed the expected high affinity (Figure 3). Analysis by electrospray MS gave a determined molecular weight of 23 583.9 Da, corresponding to the predicted molecular mass of 23 583.8 Da for an N-terminally acetylated protein: i.e. 42 Da greater than the *E. coli* expressed protein. CD measurements showed the protein to have a spectrum virtually identical to those shown in Figure 2A.

There were however a number of problems with purification of the native protein. Batches of purified protein were found which, although appearing to have the expected anomalous size on an SDS−PAGE and normal CD spectrum, did not bind to actin. These preparations were shown by MS to be composed mainly of a 23 471.2 Da species, smaller than expected by 113 Da. There was also some copurification of a second lower molecular weight band (apparent weight ca. 30 kDa by SDS) which showed some binding to actin. This was presumed to be the *TPM2* gene product (yTm2), a smaller 161-amino acid long tropomyosin also found in yeast (*2*). Together these contaminants made detailed characterization of the native protein impossible since both contaminants would influence the results of all the measurements undertaken. It should be noted that correctly folded Tms or Tm fragments would still be expected to give the same CD spectra.

Production and Expression of Modified TPM1 Constructs. The use of an N-terminal extension to mimic the acetylation present in native skeletal Tm has been investigated by several workers using a variety of peptide extensions ranging from 2 to 69 amino acids, all of which restored actin binding (*12*, *13*, *22*, *23*). However, further functional characterization of these mutants using techniques such as viscosimetry and regulation of the actomyosin ATPase have shown that many are clearly not nativelike in terms of these properties (*13*, *24*). We therefore produced N-terminally modified yTm1s using either the dipeptide extension described by Monteiro et al. (*23*) as being most nativelike in terms of viscosity, actin binding, and ATPase regulation or sequences based upon the apparent natural extension present in fibroblast Tm 5a/5b [as described by Lewis et al. (*25*) for platelet Tm]. Figure 1 shows the N-terminal sequences of yTm1, Tm 5a/5b, and yTm1 constructs produced here.

Each mutant showed similar expression levels to bacterially produced yTm1 and produced yields of 20−30 mg of protein from 1 L of cultured cells. Mass spectrometry of the constructs gave molecular weights of 23 698.4, 23 930.8, and 23 855.3 Da compared to calculated weights (lacking the N-terminal Met) of 23 699.9, 23 931.1, and 23 856.0 Da. This is consistent with previous work (*23*, *26*) which showed that for sequences in which the second amino acid is small and uncharged (Ala in all cases) the N-terminal methionine is removed posttranslationally in *E. coli* [also shown to be true for native platelet Tm (*25*)]. This gives N-terminal extensions

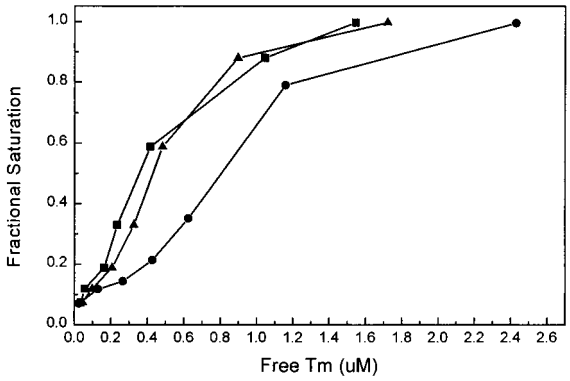

FIGURE 4: Binding curves of the three yTm1 mutants for actin determined by cosedimentation under the same conditions as stated in Figure 3. Varying concentrations of tropomyosin were mixed with 10 μM actin and then cosedimented at 100000*g* for 20 min. Binding was then determined by measurement of the concentration of free and bound tropomyosin, using quantitative scanning of Coomassie blue stained gels of the supernatant and pellet, respectively.

of 2 amino acids for yTm 1(n2) and 5 amino acids for yTm 1(n5) and yTm 1(n9), see Figure 1. In contrast, for the wild-type yTm1 sequence where the N-terminal methionine is followed by Asp, the Met is not removed in either the native form from yeast or the wild-type expressed in *E. coli*.

Tropomyosin Binding to Actin. Cosedimentation was used to measure binding to F-actin as detailed previously. Figure 3 shows that all three of the Tm constructs bind to actin. The solution conditions used are within the range known to be optimal for both yeast and vertebrate Tm binding to F-actin [see Novy et al. (*26*) and Liu et al. (*21*)]. Figure 4 shows binding curves determined for the three mutant Tms. All show the cooperative binding curves expected for Tms with little difference in the affinities of the three Tms for actin. Half-saturation points ($K_{50\%}$) were determined as 0.3 and 0.4 μM for yTm1(n2) and yTm1(n9), respectively, and 0.8 μM for yTm1(n5).

Circular Dichroism Melting Curves. The effects of the N-terminal modifications upon the stability of Tm were measured by the thermal dependence of the CD elipticity at 222 nm shown in Figure 2B. Studies were performed in a high-salt buffer (10 mM $NaPO_4$ pH 7.0, 0.5 M NaCl, 1 mM EDTA, 1 mM DTT) to prevent self-association of Tms. The initial spectra (20 °C) of each of the tropomyosins were virtually identical to those of Figure 2A indicating they were all fully folded coiled-coils. As found for other Tms, melting was fully reversible with a repeated melting curve being identical to the initial ones. yTm1 and yTm1(n2) show very similar melting curves (midpoint ≈39 °C), with yTm1(n5) and yTm1(n9) showing the initial melting and midpoints (≈41 °C) increased by around 2 °C. The cooperativity of the melting transitions is similar for all the Tms apart from yTm1(n9) which shows a slight increase in the steepness of the unfolding transition in the later part of the curve.

S1 Binding to Actin·Tm Complex. As found previously for mammalian Tms, none of the Tms showed any effect on the rate of binding of myosin S1 to actin (data not shown), indicating no occupancy of the blocked regulatory state. Equilibrium titrations were carried out under similar conditions to those previously described (*11*). For titrations containing Tm it is important that the thin filaments are saturated with Tm throughout the titration since S1 binding

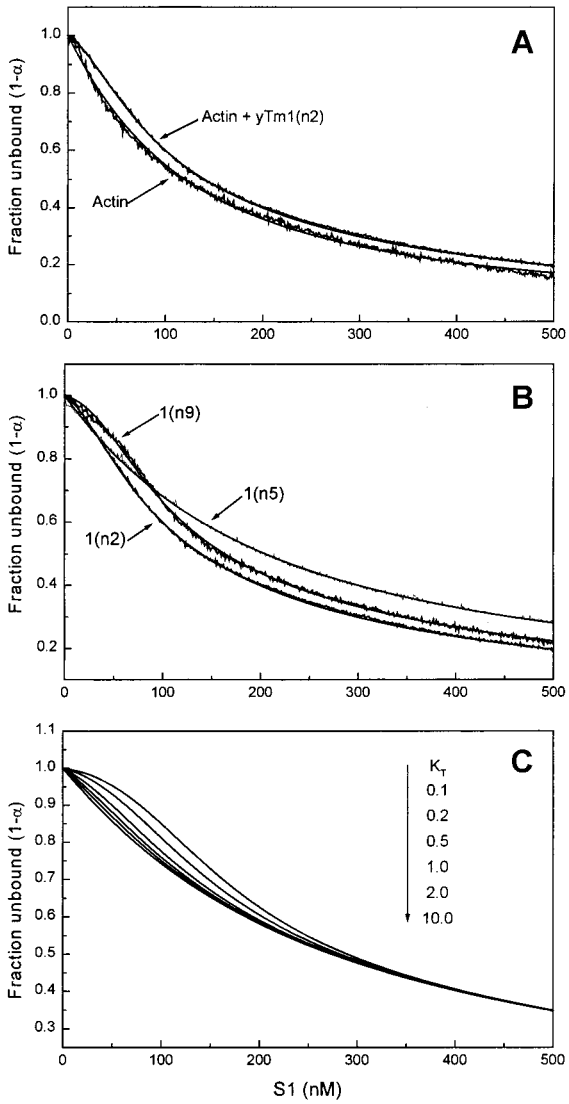

FIGURE 5: Myosin S1 binding curves to 50 nM phalloidin-stabilized pyr-actin, buffer conditions: 20 mM MOPS pH 7.0, 200 mM KCl, 5 mM $MgCl_2$. (A) actin alone compared to actin plus 2 μM yTm1-(n2). The data are shown superimposed with fitted curves to either the simple binding model (eq 1) for actin alone or the cooperative binding model (eq 3) for the sigmoidal yTm1(n2) curve. (B) Myosin S1 binding curves in the presence of 2 μM of each of yTm1 mutants. Values determined for the curve fits using eq 3 are shown in Table 1. (C) Simulations of S1 binding curves based upon values of K_1, K_2, and n for yTm1(n2) and varying values for K_T (0.1, 0.2, 0.5, 1, 2, 10).

to actin can promote Tm binding and vice versa. This would result in an uninterpretable complex curve for S1 binding to an unsaturated filament. In this respect a 2 μM concentration of Tm, well above the determined $K_{50\%}$, was used for all Tm containing titrations to ensure saturation.

Titrations of myosin S1 against 50 nM unregulated actin in the presence or absence of yTm 1(n2) are shown in Figure 5A. The binding curves are shown plotted as the fraction of unbound actin against total S1 concentration to allow easy comparison between the two. The titration of unregulated actin is fitted using the simple binding model (eq 1) which gives a determined K_d of 179 nM. The titration containing yTm1(n2) gave a sigmoid curve as expected for the cooperative binding of S1 in the presence of Tm.

Titrations of S1 against actin·Tm for each of the three mutant Tms are shown in Figure 5B. The titration curves

Table 1: Parameters for the Fits to the Binding Curves Shown in Figure 5B

parameter	yTm1(n2)	yTm1(n5)	YTm1(n9)
K_1 ($M^{-1} \times 10^4$)	4.4	2.8[a]	3.8
K_2	200	200[a]	200
K_T	0.37	>1[a]	0.14
n	9	nd[a]	8

[a] Binding curve can be fitted using a simple binding model with a K_d of 179 nM. K_1 is therefore calculated using the assumed value of K_2.

for each differ significantly. The curves for yTm1(n2) and yTm1(n9) were clearly sigmoidal and were fitted to eq 3 by a process of systematic fitting as described previously (*11*). The value of K_2 is a property of actin and myosin and hence independent of the Tm used. It was therefore fixed at the independently determined value of 200 (*27*). This allowed fitting of the parameters K_1 and K_T as the value of the apparent cooperative unit size n was varied over integer values between 4 and 11. The best fit was determined by comparison of the sum of squares, the deviation of the residuals, and the standard deviation of the fitted parameters. The results of the curve-fitting process are shown in Table 1. The fits for the yTm1(n2) and yTm1(n9) were achieved with similar best-fit values for both K_1 (4.4 and 3.8×10^4 M^{-1}, respectively) and the apparent cooperative unit size n (8 and 9, respectively). The variation between the binding curves is therefore accounted for by changes in K_T, which had values of 0.37 and 0.14. Thus for the yTm1(n2) construct the equilibrium lies further toward the open state of the filament.

The binding curve for yTm1(n5) is not significantly sigmoidal and is consistent with K_T being >1; i.e. the filament is largely in the open conformation. This data has therefore been fitted using the simple noncooperative binding model, which produces a good fit to the data. The K_d determined using this model is equivalent to the product of K_1K_2 in the cooperative model. To allow comparison the value of K_1 has been calculated using the assumed value for K_2 as shown in Table 1. The value of K_1 (2.8×10^4 M^{-1}) is similar to the value for the n2 and n9 constructs. Thus in each case the data can be well-fitted with only a change in the value of K_T

DISCUSSION

Previous to this work, yTm1 had been characterized using protein purified directly from yeast where it is present at a relatively low level [0.01%, Liu and Bretscher (*21*)]. Although overexpression of yTm1 in yeast has been reported (*1*) our own attempts at expression in yeast using a GAL promoter were unsuccessful (data not shown). However, a similar expression system gave good overproduction of yTm2 (*2*). We show here that expression of yTm1 in *E. coli* produced good yields of recombinant protein. The recombinant protein had a characteristic tropomyosin CD spectrum virtually identical to that of native skeletal Tm indicating the protein to be correctly folded. The protein has little, if any, affinity for F-actin, and mass spectrometry shows it to be unmodified. The native protein purified from yeast has been shown to bind to actin (*21*). We have purified the native protein and shown that its mass corresponds to that expected for an acetylated protein. It can therefore be concluded that the native protein is N-terminally acetylated by yeast and that this is necessary to produce a fully functional protein, as seen for skTm (*28*).

Several preparations of native yTm1 from yeast showed no binding to actin. MS analysis indicated a single major ion peak indicating the majority was proteolyzed in all cases, with a mass corresponding to an N-terminally acetylated protein which has lost the C-terminal leucine. This protein runs at the same apparent molecular weight as native protein on SDS−PAGE and shows an identical CD spectrum indicating a fully folded protein. Thus for this yTm with a correctly formed N-terminus, the loss of a single amino acid from the C-terminus has dramatic effects upon its actin-binding properties. The C-terminus is therefore as sensitive to small structural changes as the N-terminus. This result is similar to binding data for mammalian Tms lacking a larger portion of their C-terminus (*29*, *30*).

All of the N-terminal modifications produced restored actin binding to the recombinant proteins. Their affinities for actin as determined by cosedimentation were both similar to each other (50% saturation at 0.3−0.8 μM) and also to that of skTm (0.4 μM under similar conditions, data not included) showing no great difference between the constructs in terms of their actin-binding properties.

The thermal stability of the constructs shows greater variation than might have been expected. It has been stated that the N-terminus of skTm is one of the less stable portions of the molecule (*31*) and is responsible for the initial CD melting transition seen for skTm. The increased initial melting temperature of the yTm1 n5/n9 mutants in comparison to the native and n2 forms could be due to the N-terminal extensions stabilizing the N-terminus. This would, however, be in contrast to work showing that the exon 1b sequence (fibroblast Tm 5a/b, as used in the yTm1 n5/n9 constructs) has a low stability and does not form a coiled-coil under similar conditions (*32*). If the N-terminus is melting first, as might be expected, the question then arises as to how to explain the differences in the slope of the later part of the melting curves of yTm1(n5) and yTm1(n9). From these data it is difficult to equate changes in thermal stability to changes of either sequence or function within this set of mutants.

The S1 equilibrium binding titrations show that yTm can induce cooperativity in the binding of S1 to actin as for mammailian Tms. Furthermore, changes in the N-terminus do modulate the form of the cooperativity. We find that the presence of yTm on actin has little effect on the affinity of S1 for actin (K_1 and K_2) or on the apparent size of the cooperative unit (n), and the changes in the S1 binding curves are produced by changes in K_T alone.

Equilibrium Between the Closed and Open States − K_T. The values of K_T determined are within a critical range of sensitivity where relatively small changes in its value reflect significant changes in the shape of the binding curve. This is demonstrated in Figure 5C which shows simulations of S1 titration curves using yTm1(n2) values for K_1, K_2, and n as a basis and varying the value of K_T from 0.1 to 10. It can be seen that changes in K_T below 1 show the largest effect upon the shape of the curve with the sigmoidicity decreasing as the value of K_T increases. As K_T is increased above 1, the shape of the curve becomes far less sensitive to changes

in K_T and shows that the titration becomes insensitive to the value of K_T once the filament is more than around 50% in the open state.

The alteration of the structure of the N-terminus caused by addition or modification of its sequence has the ability to affect the apparent equilibrium constant for the open to closed transition. It is perhaps unexpected that such small changes in this area of the molecule, which produce Tms with otherwise similar properties such as actin binding, can have such a large effect upon regulatory function. This suggests that this region is very important not only for binding to actin and communication between adjacent Tms but also for defining the preferred conformation/binding site on the actin surface. There are two possibilities for the effect of this region upon stabilization of the open state. The first is that the changes in the overlap region are causing an overall change in the Tm conformation that alters the Tm−actin interaction. The alternative is that there are specific interactions between the overlap region and actin which alter the equilibrium between the states. In either case the energy differences between the closed and open states are low as there is little effect upon the overall actin affinity for any of the mutants. This also shows that careful characterization of Ala-Ser or other N-terminal mutants in comparison to native proteins is required before their widespread adoption as a method to produce fully nativelike Tms in *E. coli*.

Cooperative Unit Size. The apparent cooperative unit size of all of these Tms is similar (≈9, with the reservation that the unit size for yTm1(n5) cannot be explicitly determined) and almost twice that of the structural unit size of 5. Our initial expectation was that changes in the N-terminus could affect Tm−Tm contacts and alter the efficiency of communication between Tms along the actin filament. However, this appears not to be the case, and once the Tm−Tm contacts are sufficient to allow Tm binding to actin, the Tm−Tm communication is not affected. This is consistent with our view that Tm should be considered as a continuous filament with the apparent cooperative unit size being dependent upon the filament properties (*7*, *11*).

Affinity of Tm for Actin. There has been speculation that skTm consists of 7 quasi-equivalent actin-binding sites and hence the affinity should be dependent upon their length (*33*). A slightly different view of this has been proposed by Landis et al. (*34*) from their deletion studies of skeletal Tm. They suggest that Tm has a number of nonequivalent actin-binding sites, with the ends of the molecule having greater affinity for actin than the middle. An alternate view is that the majority of binding energy is due to the formation of a continuous Tm filament along the actin backbone (*35*) and the Tm−Tm contacts are essential for this. In this case the spiral structure of the Tm filament wrapped around the actin filament could be sufficient to stop dissociation without the necessity of strong direct interactions with actin.

Comparison of the midpoints of the S1 titration curves shown in Figure 5B and the fitted K_1 values shows that the presence of yTm1(n2) has only a small effect on the affinity of S1 for the thin filament. This is unlike skTm which produces a 4−7-fold increase in S1 affinity (*4*) and is caused by a decrease in k_{-1} (the rate constant of dissociation from the A state) and hence an increase in K_1 (*36*). It has recently been shown that this increase in the affinity of S1 for actin (and a reciprocal increase in Tm affinity for actin) is common to a wide range of mammalian Tm constructs (*37*). Thus the binding of Tm to actin (primarily into the closed state) occurs at a lower affinity than to an actomyosin filament (primarily the open state). This could mean that Tm binds much tighter to an open actin filament than to the closed form. However, the free energy of the open/closed transition is very small ($K_T = 0.1-1$); thus the affinities of Tm for the two states should also be very similar. The alternative is that the increase in both Tm and myosin affinities is due to a myosin−Tm interaction either directly or through actin. The observation presented here that yTm does not increase the affinity of myosin for actin suggests that this myosin−Tm interaction is absent even though the actin and myosin are the same as used for previous experiments for the skeletal system. Moraczewska et al. (*37*) suggested that the affinity of Tm for actin is related to K_T, the equilibrium constant for the closed to open switch. However the yTm constructs show little change in affinity for actin with significant variation in the value of K_T, suggesting that this relationship does not hold for yTm.

Overall this work shows that yeast Tm1 can be a valuable system to study the effects of Tm structure upon regulatory function. It has similar properties to that of mammalian Tms in its ability to regulate the myosin interactions and similarity to skTm in needing N-terminal modification to promote actin binding. But it also has differences to mammalian Tms, especially in terms of the promotion of myosin binding to actin, which help shed further light upon the regulatory process. Finally its small size is advantageous in measurements of apparent cooperativity and will be useful in future structural studies.

ACKNOWLEDGMENT

We thank Sam Lehrer for his helpful discussion and Nancy Adamek for protein preparations.

REFERENCES

1. Liu, H. P., and Bretscher, A. (1989) *Cell 57*, 233−42.
2. Drees, B., Brown, C., Barrell, B. G., and Bretscher, A. (1995) *J. Cell. Biol. 128*, 383−92.
3. Pruyne, D. W., Schott, D. H., and Bretscher, A. (1998) *J. Cell. Biol. 143*, 1931−45.
4. Greene, L. E., and Eisenberg, E. (1980) *Proc. Natl. Acad. Sci. U.S.A. 77*, 2616−20.
5. Hill, T. L., Eisenberg, E., and Greene, L. (1980) *Proc. Natl. Acad. Sci. U.S.A. 77*, 3186−90.
6. McKillop, D. F., and Geeves, M. A. (1993) *Biophys. J. 65*, 693−701.
7. Lehrer, S. S., Golitsina, N. L., and Geeves, M. A. (1997) *Biochemistry 36*, 13449−54.
8. Schaertl, S., Lehrer, S. S., and Geeves, M. A. (1995) *Biochemistry 34*, 15890−4.
9. Ishii, Y., and Lehrer, S. S. (1990) *Biochemistry 29*, 1160−6.
10. Vibert, P., Craig, R., and Lehman, W. (1997) *J. Mol. Biol. 266*, 8−14.
11. Maytum, R., Lehrer, S. S., and Geeves, M. A. (1999) *Biochemistry 38*, 1102−10.
12. Hitchcock-DeGregori, S. E., and Heald, R. W. (1987) *J. Biol. Chem. 262*, 9730−5.
13. Urbancikova, M., and Hitchcock-DeGregori, S. E. (1994) *J. Biol Chem. 269*, 24310−5.
14. Maytum, R., Konrad, M., and Geeves, M. A. (1998) *Biophys. J. 74*, A53.

15. Sambrook, J., Fritsh, E., and T. M. (1989) *Molecular Cloning A Laboratory Manual*, 2nd ed., Cold Spring Harbor Laboratory, Cold Spring Harbor, NY.
16. Konrad, M. (1993) *J. Biol. Chem. 268*, 11326−34.
17. Weeds, A. G., and Taylor, R. S. (1975) *Nature 257*, 54−6.
18. Spudich, J. A., and Watt, S. (1971) *J. Biol. Chem. 246*, 4866−71.
19. Criddle, A. H., Geeves, M. A., and Jeffries, T. (1985) *Biochem. J. 232*, 343−9.
20. Laemmli, U. (1970) *Nature 227*, 680−85.
21. Liu, H. P., and Bretscher, A. (1989) *Proc. Natl. Acad. Sci. U.S.A. 86*, 90−3.
22. Heald, R. W., and Hitchcock-DeGregori, S. E. (1988) *J. Biol. Chem. 263*, 5254−9.
23. Monteiro, P. B., Lataro, R. C., Ferro, J. A., and Reinach, F. d. C. (1994) *J. Biol. Chem. 269*, 10461−6.
24. Cho, Y. J., Liu, J., and Hitchcock-DeGregori, S. E. (1990) *J. Biol. Chem. 265*, 538−45.
25. Lewis, W. G., Cote, G. P., Mak, A. S., and Smillie, L. B. (1983) *FEBS Lett. 156*, 269−73.
26. Novy, R. E., Liu, L. F., Lin, C. S., Helfman, D. M., and Lin, J. J. (1993) *Biochim. Biophys. Acta 1162*, 255−65.
27. McKillop, D. F., and Geeves, M. A. (1991) *Biochem. J. 279*, 711−8.
28. Kluwe, L., Maeda, K., Miegel, A., Fujita-Becker, S., Maeda, Y., Talbo, G., Houthaeve, T., and Kellner, R. (1995) *J. Muscle Res. Cell. Motil. 16*, 103−10.
29. Heeley, D. H., Golosinska, K., and Smillie, L. B. (1987) *J. Biol. Chem. 262*, 9971−8.
30. Hammell, R. L., and Hitchcock-DeGregori, S. E. (1996) *J. Biol. Chem. 271*, 4236−42.
31. Greenfield, N. J., Stafford, W. F., and Hitchcock-DeGregori, S. E. (1994) *Protein Sci. 3*, 402−10.
32. Greenfield, N. J., Palm, T., Monleon, D., Montelione, G. T., and Hitchcock-DeGregori, S. E. (2000) *Biophys. J. 78*, A399.
33. Hitchcock-DeGregori, S. E., and Varnell, T. A. (1990) *J. Mol. Biol. 214*, 885−96.
34. Landis, C., Back, N., Homsher, E., and Tobacman, L. S. (1999) *J. Biol. Chem. 274*, 31279−85.
35. Cote, G. P. (1983) *Mol. Cell. Biochem. 57*, 127−46.
36. Geeves, M. A., and Halsall, D. J. (1987) *Biophys. J. 52*, 215−20.
37. Moraczewska, J., Nicholson-Flynn, K., and Hitchcock-DeGregori, S. E. (1999) *Biochemistry 38*, 15885−92.

BI000977G